Periprosthetic stress shielding in patello-femoral arthroplasty: a numerical analysis

Bernardo Innocenti[1], Hans-Peter W. van Jonbergen[2], Luc Labey[1] and Nico Verdonschot[3,4]

1 European Centre for Knee Research, Smith&Nephew, Leuven, Belgium
2 Department of Orthopedic Surgery, Deventer Hospital, The Netherlands
3 Laboratory for Biomechanical Engineering, University of Twente, Enschede, The Netherlands
4 Orthopaedic Research Laboratory, Radboud University Nijmegen Medical Centre, Nijmegen, The Netherlands

Abstract: Total knee replacement gives proven good results for isolated patello-femoral osteoarthritis, but patello-femoral arthroplasty may be more appropriate because only the joint compartment is replaced. Although the femoral component of a patello-femoral prosthesis is smaller than in total knee arthroplasty, it is unknown whether strain-adaptive periprosthetic bone remodeling occurs following patello-femoral arthroplasty. The aim of the study was to evaluate and compare the stress shielding effect of prosthetic replacement with Finite Element (FE) modeling. Four FE models were developed to investigate the effects of different patellofemoral replacement designs; we compared the stress shielding effect in the distal femur between a physiological model of knee, the Richards type II patellofemoral prosthesis, the Journey PFJ prosthesis, and the Genesis II total knee prosthesis. The geometry of the knee joint was obtained from a MRI of a patient. Von Mises stress was evaluated in the same regions of interest as in the experimental analysis, during a loaded squat until 120° of flexion, similar to previous experimental tests performed on knee kinematics simulators. During knee flexion the Journey PFJ has a similar trend of the physiological knee; the Richards II PFJ has higher stress shielding than the other PFJ model and in the Genesis II TKA the stress shielding is higher compared to the PFA models. The results agree with experimental DXA literature results; in particular they demonstrated that, during knee flexion, the magnitude of the Von Mises stress behind the anterior flange was about the same for the physiological model and for the Journey PFJ but smaller for the Richards II. This stress shielding effect of the Richards II was most obvious around 90 degrees of flexion. This phenomenon can possibly be explained by the particular design features of the Richards II. In the proximal region of the bone the values of the Von Mises stress were about the same magnitude for the physiological model and for both patello-femoral prostheses and also these findings are in agreement with the experimental DXA outcome.

Keywords: Biomedics, Implantable Medical Device, Patellofemoral joint; Stress shielding; Squat movement

Visit the SIMULIA Resource Center for more customer examples.

1. Introduction

Total knee arthroplasty gives predictable good results for isolated patellofemoral osteoarthritis (Dejour et al. 2004, Dalury 2005, Meding et al. 2007). However, a less aggressive approach using patellofemoral arthroplasty may be more appropriate. Using this approach, in contrast with total knee arthroplasty, only the involved joint compartment is replaced and the femorotibial joint remain intact, thus probably inducing a more physiologic joint motion.

The long-term outcome of patellofemoral arthroplasty is related to progression of femorotibial osteoarthritis and the need for conversion to total knee arthroplasty (van Jonbergen et al. 2010b). The results of conversion to total knee arthroplasty may be compromised by loss of bone behind the prosthesis. In total knee arthroplasty, loss of bone stock occurs due to the stress shielding effect of the femoral component (Tissakht et al. 1996, Van Lenthe et al. 1997). Although the femoral component of patellofemoral prosthesis is smaller than in total knee arthroplasty, it is unknown whether strain-adaptive periprosthetic bone remodeling occurs following patellofemoral arthroplasty.

Finite element analyses have been used extensively in the evaluation of prosthetic load, stress distribution in the bone and bone remodeling after total hip and knee replacement (Qian et al. 2009, Zelle et al. 2009). Some investigators have also used numerical models to calculate the stress distribution within the patellar components after patellofemoral replacement (Najarian et al. 2005, Morra and Greenwald 2006). However, none of these models analyze a loaded distal femur during a squat to investigate the effect of the femoral component on the stress distribution in the periprosthetic bone.

The objective of this study was to evaluate and compare the stress shielding effect of prosthetic replacement with Finite Element (FE) modeling. For this purpose, a patellofemoral joint was modeled with and without a patellofemoral joint replacement. Moreover, to investigate the effects of different patellofemoral replacement designs, we compared two patellofemoral prostheses and with one total knee prosthesis.

2. Methods

2.1 Physiological Knee joint geometry

MR imaging data from the right knee of a healthy old volunteer without any known musculoskeletal disease were manually segmented to obtain a three-dimensional model of the osseous and cartilaginous geometries of distal femur and patella with patellar tendon and insertion of the quadriceps tendon (Figure 1).

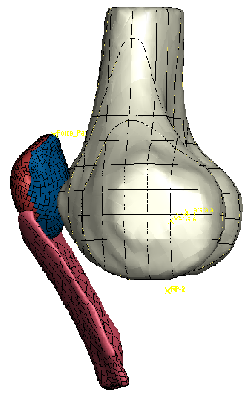

Figure 1. Physiological model geometries used in this study.

2.2 Knee Joint material properties

According to previous literature study (Heegaard et al. 2001, Beillas et al. 2004) the trabecular bone was modeled as a homogenous isotropic linear elastic material (E=300 MPa, Poisson ratio v=0.30, and a density of 1g/cm^3) while the cortical bone was modeled as an orthotropic 2mm thick layer (E1 = 17900MPa, E2 = 18800 MPa, E3 = 22800, G23 = 7110 MPa, G31 = 6580 MPa, G12 = 5710 MPa). The patella was modeled as a homogenous isotropic linear elastic material (E=15000 MPa, Poisson ratio v=0.30, density= 2g/cm^3) with a 2.5mm thick layer of homogenous isotropic linear elastic cartilage (E=5 MPa, Poisson ratio v=0.46, and a density of 1g/cm^3) in contact with the femoral trochlea (Beillas et al. 2004, Iranpour et al. 2008, Pena et al. 2005, Pena et al. 2006). The friction coefficient between patella and trochlear groove was set at 0.001 based on experimental data (Besier et al. 2005). The patellar tendon was modeled as an isotropic and hyperelastic material (Pena et al. 2005, Weiss et al. 2001), with rubber-like mechanical behavior.

2.3 Knee Joint load and constraints

The simulated motion consisted of a 10s loaded full squat (one cycle), starting from 0° until a maximum flexion angle of 120°. These settings match the experimental kinematics simulations performed in a previous *in vitro* analysis on physiological cadaver legs (Innocenti et al. 2009, Victor et al. 2009, Victor et al. 2010). The patella model was constrained by fixing the distal part of the patellar ligament and applying a quadriceps force distributed on the quadriceps insertion on the proximal surface of the patella. Thus, the patella was allowed to move along the trochlear surface of the femur (Sharma et al. 2008). The magnitude and direction of the quadriceps force as well as the 3D kinematics were applied using the Grood-Suntay coordinate system (Figure 2) (Grood and Suntay 1983), using as origin the midpoint between the condylar center (Innocenti et al. 2009, Victor et al. 2009, Victor et al. 2010).

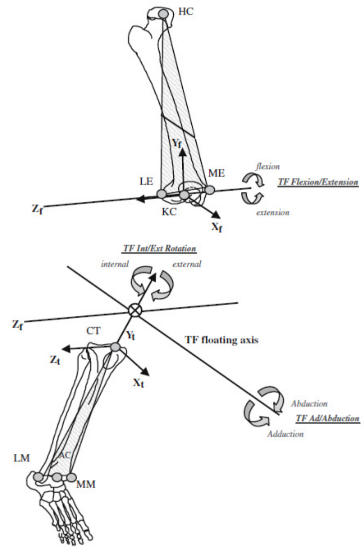

Figure 2. the Grood-Suntay coordinate system used to describe the 3D kinematics.

2.4 Physiological knee joint finite element model

The three-dimensional models of femur, patella and patellar tendon were imported in commercially available finite element analysis software (Abaqus 6.8EF-1, Dassault Systemes Simulia, Providence, RI, USA). The models were meshed with 2 mm 6-noded triangle elements for the cortical and cartilage layers, and 2 mm 10-noded tetrahedral elements for the trabecular bone, patellar bone and patellar ligament. A convergence analysis was used to validate mesh adequacy. Two regions of interest (ROI) were defined in the femoral bone: an anterior and a proximal ROI (Figure 3). The location of the ROIs was defined to fit the same regions as used in a previous bone mineral density analysis following patellofemoral arthroplasty (van Jonbergen et al. 2010a). The ROIs were 1 cm high in femoral proximo-distal direction and 1 cm long in the anteroposterior direction. They spanned the entire medio-lateral width. During the dynamic simulation the average Von Mises stress in each ROI was calculated.

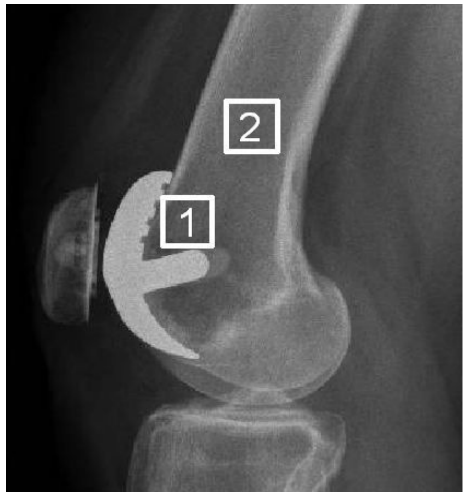

Figure 3. Position of the Region of Interest (ROI): 1 anterior ROI, 2 superior ROI

2.5 Patello femoral finite element models

Two patello femoral prosthesis were considered in this study: Journey PFJ femoral component (Smith&Nephew, Memphis, TN) and the Richards II patellofemoral prosthesis (Smith&Nephew, Memphis, TN) (Figure 4 and Figure 4). The geometries of the prosthetic components were taken from CAD files provided by the manufacturer and both implants were incorporated in the knee model following the manufacturers' instructions.

The Journey PFJ femoral component, in Oxinium™, was modeled as an isotropic linear elastic material (E=97905 MPa, Poisson ratio v=0.3, density=6.62 g/cm^3) (Zirconium Products: Technical Data Sheet 2003) while the Richards II femoral component, in CoCr, was modeled as an isotropic linear elastic material (E=240000 MPa, Poisson ratio v=0.3) (Davis 2003). The UHMWPE patellar component was modeled as a non-linear elasto-plastic material (E=684.65 MPa, Poisson ratio v=0.45) (Godest et al. 2002, Halloran et al. 2005, Innocenti et al. 2009). A 2mm cement layer with linear elastic material properties (E=3000 MPa, Poisson ratio v=0.3) was modeled between the prosthetic components and the cut bone surfaces (Janssen et al. 2008, Vaninbroukx et al. 2009). The frictional coefficient between the patellar component and the femoral component was set at 0.04 based on experimental data (Poggie et al. 1992).

The models were meshed with 2 mm 6-noded triangle elements for the cortical bone and cement layers, and 2 mm 10-noded tetrahedral elements for the cancellous bone, patellar bone, femoral component, patellar component and patellar ligament. A convergence analysis was used to validate mesh adequacy.

We defined an anterior and a posterior ROI in the same positions and with the same dimensions as in the physiological model. During the dynamic simulation the average Von Mises stress in each ROI was recorded as a function of time and flexion angle.

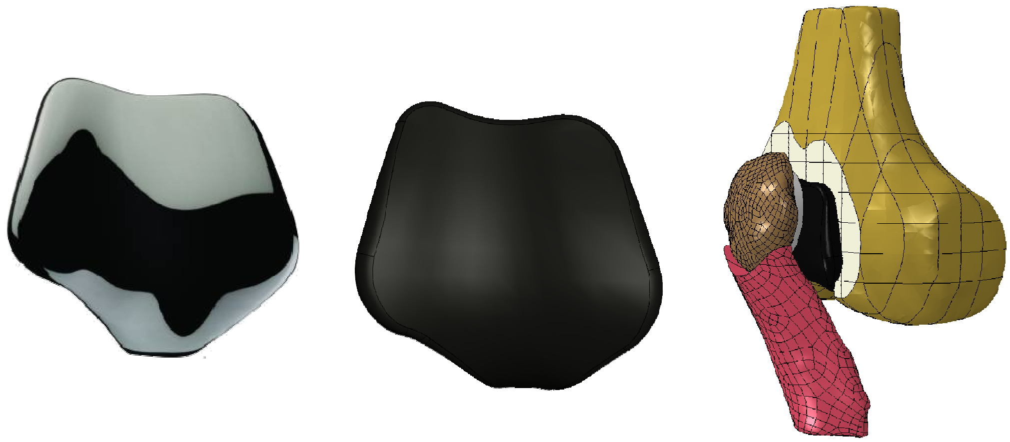

A) B) C)

Figure 4. Journey PFJ Prosthesis: A) Real Component, B) CAD file, C) Finite Element Model

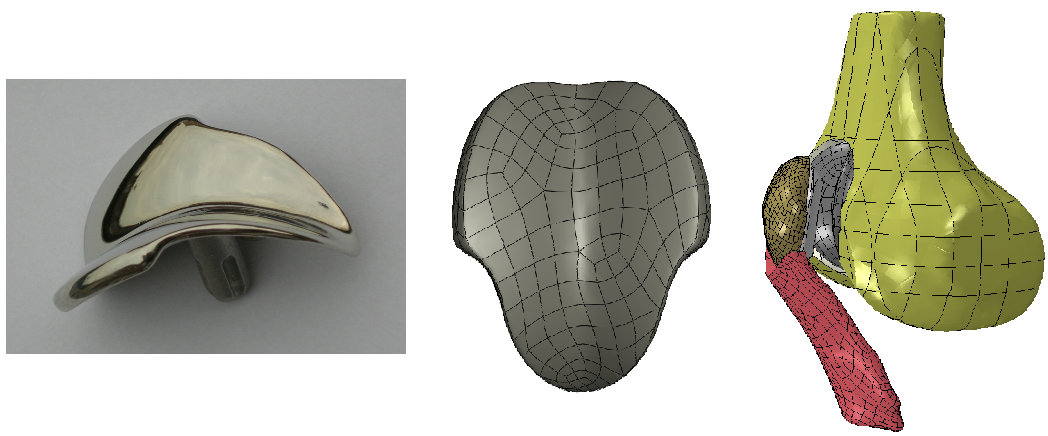

A) B) C)

Figure 5. Richards II Prosthesis: A) Real Component, B) CAD file, C) Finite Element Model

2.6 Genesis II total knee prosthesis finite element model

The geometries of the prosthetic components were taken from CAD files provided by the manufacturer (Figure 6). The implants were incorporated in the knee model following the manufacturers' instructions.
The models were meshed with 2 mm 6-noded triangle elements for the cortical bone and cement layers, and 2 mm 10-noded tetrahedral elements for the cancellous bone, patellar bone, femoral component, patellar component and patellar ligament. A convergence analysis was used to validate mesh adequacy.
We defined an anterior and a posterior ROI in the same positions and with the same dimensions as in the physiological model. During the dynamic simulation the average Von Mises stress in each ROI was recorded as a function of time and flexion angle.

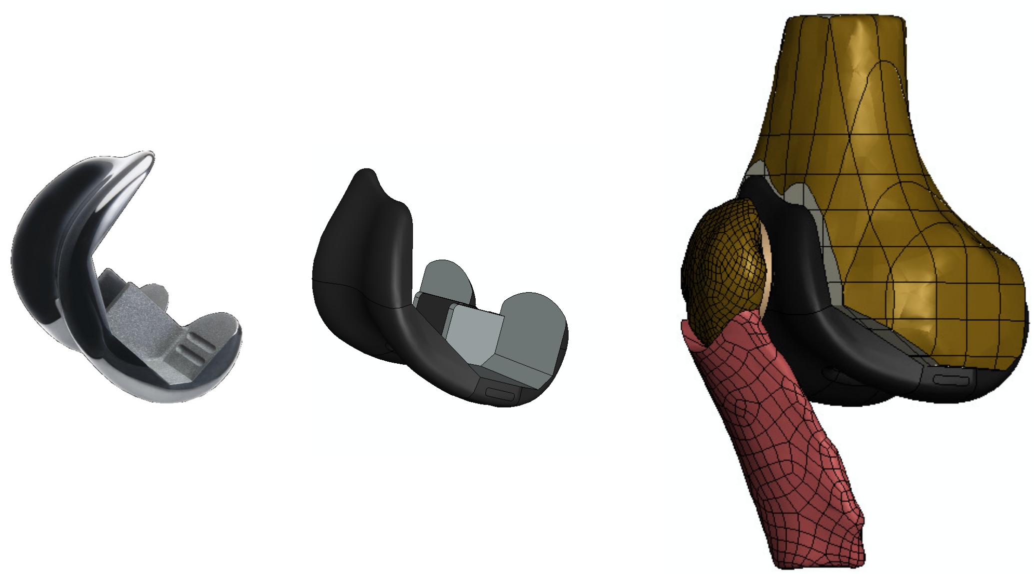

A) B) C)

Figure 6. Genesis II Prosthesis: A) Real Component, B) CAD file, C) Finite Element Model

3. Results

Figures 7 and 8 show the average Von Mises stress in the anterior and proximal ROIs, induced by the patellofemoral load, in the 4 models estimated by the dynamic finite element simulation as a function of flexion angle. Overall, the average Von Mises stress in both ROIs increased with the flexion angle. Maximum values of 2.8-3.8 MPa were reached at 90° flexion angle for the anterior ROI, and 1.4-1.6 MPa for the proximal ROI.

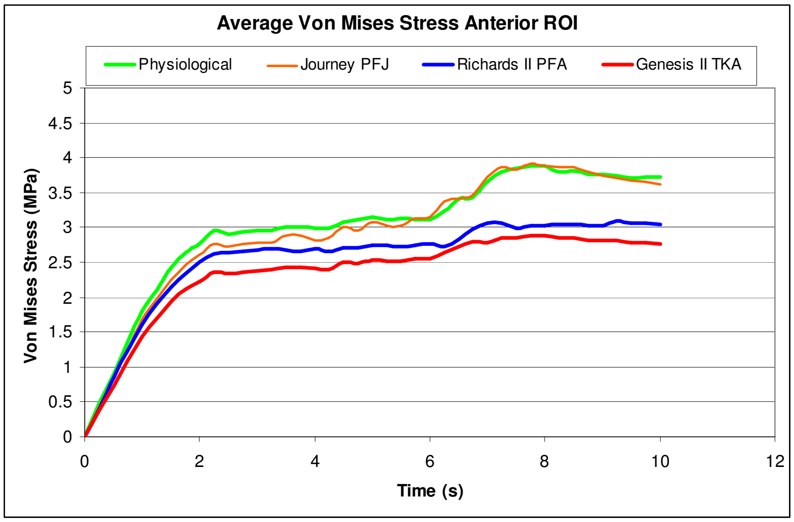

Figure 7. Average Von Mises stress in the anterior ROI in the four models as a function of time.

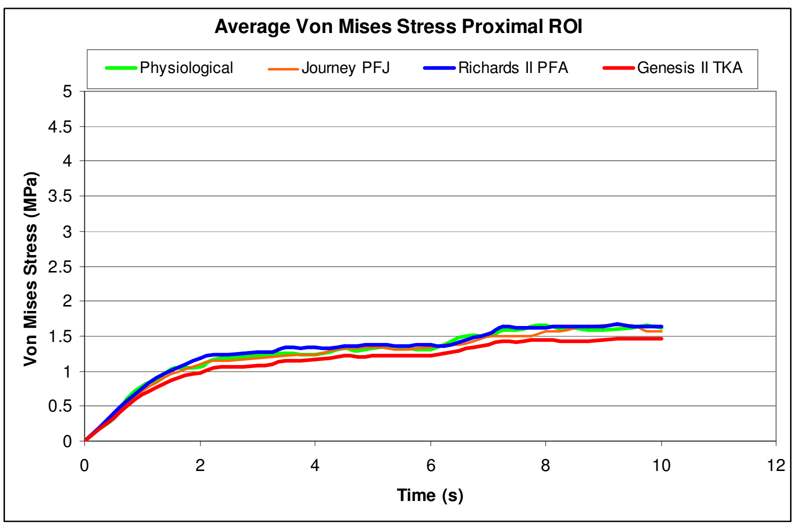

Figure 8. Average Von Mises stress in the superior ROI in the four models as a function of time.

During knee flexion from 80° till 120°, the average Von Mises stresses in the anterior ROI with the Journey PFJ design were comparable to the physiological knee. The Richards II design demonstrated lower average Von Mises stress in the anterior ROI compared to the physiological knee, and the Genesis II total knee design demonstrated the lowest average Von Mises stress. The lower average Von Mises stress in the Richards II design was most pronounced at 90 degrees of flexion.

The average Von Mises stress in the proximal ROI was similar for both patellofemoral designs and the physiological model, with slightly lower average Von Mises stress for the Genesis II total knee prosthesis.

4. Discussion

Our dynamic finite element modeling demonstrated comparable Von Mises stress in the anterior region of interest for the Journey PFJ design and the physiological knee. The Richards II design demonstrated lower average Von Mises stress in the anterior region of interest compared to the physiological knee, and the Genesis II total knee design demonstrated the lowest average Von Mises stress. The average Von Mises stress in the proximal region of interest were similar for both patellofemoral designs and the physiological model, with slightly lower average Von Mises stress for the Genesis II total knee prosthesis.

Stress shielding behind the anterior flange of a patellofemoral prosthesis may result in strain-adaptive bone remodeling with resulting decrease in bone mineral density. Our Journey PFJ model predicted no significant stress shielding, implying that the physiological strains are maintained. However, the Richards II model predicted a reduction in average Von Mises stress compared to the physiological model. This is in agreement with the recently reported results of clinical dual-energy X-ray absorptiometry (DXA) measurements obtained in 14 patients (van Jonbergen et al. 2010a). In this prospective 1-year DXA study a 15% decrease in bone mineral density was found behind the anterior flange of the Richards type II patellofemoral prosthesis.

The observed differences in the stress shielding effect between the Richards II and Journey PFJ prosthesis may result from differences in both material and geometrical properties.

The curve of the average Von Mises stress in the anterior ROI for the Journey PFJ prosthesis features a gradual transition from the Richards II prosthesis curve (from extension to early flexion) to the physiological curve (between early flexion and deep flexion) (Figure 7). This transition can be explained most probably by the fact that the Journey PFJ femoral component is shorter in the sagital plane than the Richards II component. As a result, in deep flexion the patellar button contacts the native femoral surface beyond 90 degrees of flexion while in the Richards II design there is still contact between the femoral component and the patellar button. Moreover the Richards II patellar and femoral components are highly congruent, forcing the patellar component to remain within the femoral component medio-laterally within the entire flexion range.

The present study is the first to specifically evaluate for the stress-shielding effect of a patellofemoral prosthesis. However, correct interpretation of results obtained from numerical models requires careful consideration of several important issues (Viceconti et al. 2005). We employed a numerical model that has been both verified and validated. Moreover, the biological findings based on clinical DXA measurements behind the anterior flange of the Richards II patellofemoral prosthesis (van Jonbergen et al. 2010a) match the findings of this finite element analysis. Of course, validation will only be complete by adding clinical DXA measurements in the same ROIs for the other types of implant that were considered in this simulation. This information is not available yet but it is the subject of an ongoing study.

Finite element modeling is, however, subject to limitations due to inherent uncertainties concerning geometry, load situation, and material properties. We performed our modeling using a dynamic loaded squat instead of a gait cycle which is a more frequent activity. However, we prefer squatting because it has an increased range of motion and high patello-femoral loads and thus, in our opinion, gives a better view on differences in stress distributions between different implants types. Nevertheless, analysis of other activities will probably lead to similar relative results but in a smaller range of knee flexion and with smaller differences in periprosthetic Von Mises stress values.

In this study we didn't check the stress in the interface bone-implant. Although less stress shielding means better load transfer to the bone, which is desirable, it may also imply higher loads in the interface region and an increased risk for failure of the fixation that was not considered in the present analysis.

The use of a validated finite element knee model with patellofemoral prosthesis may lead to an increased understanding of the effect of design characteristics on outcomes. Furthermore, employing a numerical model may resolve some potentially important issues pertaining to the alignment of the prosthesis such as external rotation of the trochlear component and trochlear groove orientation.

5. Conclusions

Dynamic finite element analyses of knee models with a patellofemoral joint replacement predict a decrease in strain energy density behind the anterior flange of the femoral component. This reduction was more pronounced in the Richards II design than in the Journey PFJ design, and may be related to specific design properties.

6. References

1. Beillas, P., Papaioannou, G., Tashman, S., Yang, K.H., 2004. A new method to investigate in vivo knee behavior using a finite element model of the lower limb. J. Biomech. 37, 1019-30.
2. Besier, T.F., Gold, G.E., Beaupre, G.S., Delp, S.L., 2005. A modeling framework to estimate patellofemoral joint cartilage stress in vivo. Med. Sci. Sports Exerc. 37, 1924-30.
3. Dalury, D.F., 2005. Total knee replacement for patellofemoral disease. J Knee Surg 18, 274-7.
4. Davis, J. R., 2003. Handbook of Materials for Medical Devices. ASM International, Materials Park, Ohio, USA.
5. Dejour, D., Barbosa, J., Jacquot, N., Neyret, P., 2004. Résultats des prothèses totales du genou dans l´arthrose fémoro-patellaire isolée. Rev Chir Orthop 90, 1S111-3.
6. Godest, A.C., Beaugonin, M., Haug, E., Taylor, M., Gregson, P.J., 2002. Simulation of a knee joint replacement during a gait cycle using explicit finite element analysis. J. Biomech. 35, 267-75.
7. Grood, E.S., Suntay, W.J., 1983. A joint coordinate system for the clinical description of three-dimensional motions: application to the knee. J. Biomech. Eng. 105, 136-44.
8. Halloran, J.P., Petrella, A.J., Rullkoetter, P.J., 2005. Explicit finite element modeling of total knee replacement mechanics. J. Biomech. 38, 323-31.

9. Heegaard, J.H., Leyvraz, P.F., Hovey, C.B., 2001. A computer model to simulate patellar biomechanics following total knee replacement: the effects of femoral component alignment. Clin. Biomech. (Bristol, Avon) 16, 415-23.
10. Innocenti, B., Truyens, E., Labey, L., Wong, P., Victor, J., Bellemans, J., 2009. Can medio-lateral baseplate position and load sharing induce asymptomatic local bone resorption of the proximal tibia? A finite element study. J. Orthop. Surg. Res. 4, 26.
11. Iranpour, F., Merican, A.M., Amis, A.A., Cobb, J.P., 2008. The width:thickness ratio of the patella: an aid in knee arthroplasty. Clin. Orthop. Relat. Res. 466, 1198-203.
12. Janssen, D., Mann, K.A., Verdonschot, N., 2008. Micro-mechanical modeling of the cement-bone interface: the effect of friction, morphology and material properties on the micromechanical response. J. Biomech. 41, 3158-63.
13. Meding, J.B., Wing, J.T., Keating, E.M., Ritter, M.A., 2007. Total knee arthroplasty for isolated patellofemoral arthritis in younger patients. Clin Orthop 464, 78-82.
14. Morra, E.A., Greenwald, A.S., 2006. Patellofemoral replacement polymer stress during daily activities: a finite element study. J. Bone Joint Surg. Am. 88 (Suppl 4), 213-6.
15. Najarian, S., Rostami, M., and Rezaei, T., 2005. Biomechanical analysis of patellofemoral joint prosthesis using finite element method. Proceedings of the Second IASTED International Conference.
16. Pena, E., Calvo, B., Martinez, M.A., Doblare, M., 2006. A three-dimensional finite element analysis of the combined behavior of ligaments and menisci in the healthy human knee joint. J. Biomech. 39, 1686-701.
17. Pena, E., Calvo, B., Martinez, M.A., Palanca, D., Doblare, M., 2005. Finite element analysis of the effect of meniscal tears and meniscectomies on human knee biomechanics. Clin. Biomech. (Bristol, Avon) 20, 498-507.
18. Poggie, R.A., Wert, J.J., Mishra, A.K., Davidson, J.A. Friction and wear characterization of UHMWPE in reciprocating sliding contact with Co-Cr, Ti-6Al-4V and zirconia implant bearing surfaces. In: Denton, R., Keshavan, M.K. (Eds.), Wear and Friction of Elastomers, ASTM STP 1145. pp 65-81.
19. Qian, J.G., Song, Y.W., Tang, X., Zhang, S., 2009. Examination of femoral-neck structure using finite element model and bone mineral density using dual-energy X-ray absorptiometry. Clin. Biomech. (Bristol, Avon) 24, 47-52.
20. Sharma, A., Leszko, F., Komistek, R.D., Scuderi, G.R., Cates, H.E., Jr., Liu, F., 2008. In vivo patellofemoral forces in high flexion total knee arthroplasty. J. Biomech. 41, 642-8.
21. Tissakht, M., Ahmed, A.M., Chan, K.C., 1996. Calculated stress-shielding in the distal femur after total knee replacement corresponds to the reported location of bone loss. J. Orthop. Res. 14, 778-85.
22. van Jonbergen, H.P.W., Koster, K., Labey, L., Innocenti, B., van Kampen, A., 2010a. Distal femoral bone mineral density decreases following patellofemoral arthroplasty: 1-year follow-up study of 14 patients. BMC. Musculoskelet. Disord. 11, 74.
23. van Jonbergen, H.P.W., Poolman, R.W., van Kampen, A., 2010b. Isolated patellofemoral osteoarthritis: A systematic review of treatment options using the GRADE approach. Acta Orthop. 81, 199-205.

24. van Jonbergen, H.P.W., Werkman, D.M., Barnaart, L.F., van Kampen, A., 2010c. Long-Term Outcomes of Patellofemoral Arthroplasty. J. Arthroplasty. in press.

25. Van Lenthe, G.H., de Waal Malefijt, M.C., Huiskes, R., 1997. Stress shielding after total knee replacement may cause bone resorption in the distal femur. J. Bone Joint Surg. Br. 79, 117-22.

26. Vaninbroukx, M., Labey, L., Innocenti, B., Bellemans, J., 2009. Cementing the femoral component in total knee arthroplasty: which technique is the best? Knee. 16, 265-8.

27. Viceconti, M., Olsen, S., Nolte, L.P., Burton, K., 2005. Extracting clinically relevant data from finite element simulations. Clin. Biomech. (Bristol, Avon) 20, 451-4.

28. Victor, J., Labey, L., Wong, P., Innocenti, B., Bellemans, J., 2010. The influence of muscle load on tibiofemoral knee kinematics. J. Orthop. Res. 28, 419-28.

29. Victor, J., Van Glabbeek, F., Vander Sloten, J., Parizel, P.M., Somville, J., Bellemans, J., 2009. An experimental model for kinematic analysis of the knee. J. Bone Joint Surg. Am. 91 (Suppl 6), 150-63.

30. Weiss, J., Gardiner, J.C., 2001. Computational modeling of ligament mechanics. Crit. Rev. Biomed. Eng. 29, 1-70.

31. Zelle, J., Van der Zanden, A.C., De Waal, M.M., Verdonschot, N., 2009. Biomechanical analysis of posterior cruciate ligament retaining high-flexion total knee arthroplasty. Clin. Biomech. (Bristol, Avon) 24, 842-9.

32. Zirconium Products: Technical Data Sheet. Wah Chang: An Allegheny Technologies Company. Available at: http://www.wahchang.com/pages